Robust Autonomous Aerobraking Strategies

Thomas Chabot, Guillaume Bonnéry, Saturnino Val Serra, Steve Kemble*
Astrium Satellites
**e-mail: thomas.chabot@astrium.eads.net*

Héloïse Scheer
Astrium Space Transportation

François Forget
Laboratoire de Météorologie Dynamique

Thomas Voirin, Sohrab Salehi, Daniele Gherardi
ESTEC, European Space Agency

Abstract

Although very beneficial in terms of propellant mass and a mission-enabler, aerobraking is inherently a long, hazardous and costly mission phase. Autonomy is a way to mitigate those issues and increase overall aerobraking robustness. Several topics have been identified as key for the success of future autonomous aerobraking missions and are investigated in this paper: an AOCS mode dedicated to the aerobraking phase; onboard algorithms aiming at predicting the timing of future atmospheric passes (autonomy level 1); onboard algorithms for autonomous corridor control (autonomy level 2); and finally procedures and onboard algorithms ensuring spacecraft safety, in particular in case of thermal alarm or in case of a switch to safe mode during aerobraking. The algorithms and methods proposed in this paper have been extensively validated and assessed thanks to a high-fidelity aerobraking simulator. This work was performed in the frame of European Space Agency (ESA) study "Robust Autonomous Aerobraking Strategies" (contract No. 4000102049).

1. Aerobraking, a mission-enabling but challenging technique

Aerobraking is an aero-assist technique that allows significant reduction of propellant mass on missions to planets with atmospheres, typically Mars and Venus. It consists in using the braking effect of atmospheric drag over a series of periapsis passes in order to reduce the spacecraft orbit energy and therefore its orbital period and apoapsis altitude until the operational orbit is reached. The total propellant mass gain with respect to a fully propulsive planetary orbit insertion manoeuvre can be huge, typically around 300kg for Mars missions. Aerobraking has been successfully performed by Mars Global Surveyor, Mars Odyssey and Mars Reconnaissance Orbiter US missions. An aerobraking experiment is considered in 2014 for the Venus Express mission developed by Astrium, which will allow improving the operational experience in Europe, enabling the use of aerobraking on future missions to Mars.

Although very beneficial in terms of propellant mass, aerobraking is inherently a hazardous phase since it repeatedly exposes the spacecraft to atmospheric heat flux, risking over-heating of a spacecraft component (typically solar arrays which are the main drag area), or even mission loss. Aerobraking is also a long mission phase, of typically a few months, during which ground involvement is very high including mission critical activities such as orbit restitution and prediction, atmospheric conditions monitoring and prediction, manoeuvre decision-making, etc. under tightening time constraints. This heavy workload not only has a high cost that offsets the launch cost savings of aerobraking, but also increases the risk of human error [1]. Furthermore, US experience [2] has shown that atmospheric variability quickly turns ground-based operational sequences obsolete, imposing frequent ground updates in order to keep a correct matching between sequences and actual orbit events. Autonomy is a way to mitigate those issues and increase overall aerobraking robustness. This paper presents algorithms and methods that have been designed in order to increase the autonomy level of the aerobraking phase.

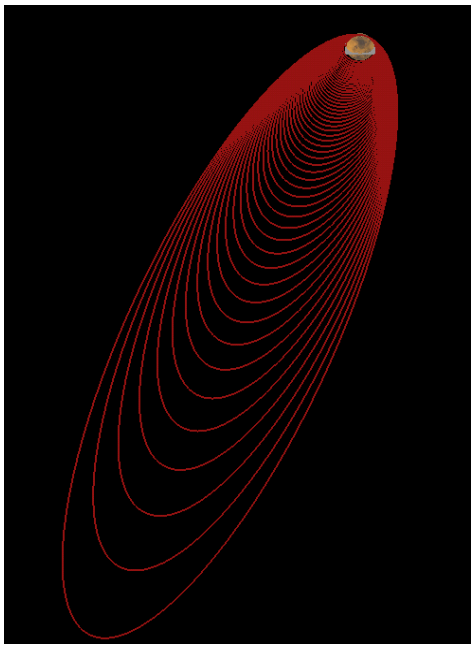

Figure 1: Typical aerobraking trajectory

In a first autonomy level, the operational sequences that are generated by the ground and uplinked to the spacecraft are autonomously corrected by the onboard Periapsis Time Estimator (PTE). Thanks to onboard accelerometer measurements, the PTE estimates the date of last periapsis and the corresponding atmospheric drag ΔV, predicts the date of next periapsis and shifts accordingly the upcoming operational sequences. In this way the required frequency of ground updates is decreased, relaxing the pressure on ground teams.

In a second autonomy level, onboard algorithms are proposed in order to perform additional activities onboard. These activities include operational sequence generation based on a simple onboard navigation approach combined with ground updates, and autonomous corridor control. The latter consists in boost manoeuvre at apoapsis decision-making and computation in order to control the periapsis altitude and therefore the heat flux and dynamic pressure experienced by the spacecraft, within an upper limit defined by thermal constraints and a lower limit defined by aerobraking strength. In this way, ground teams are relieved from most frequent and repetitive activities and may focus on higher-level activities such as monitoring the overall aerobraking progress, updating atmospheric and spacecraft models, atmosphere monitoring and aerobraking corridor tuning. The aerobraking corridor is illustrated on Figure 2 below.

A last major point of interest is the management of contingencies. On-board monitoring of critical parameters (such as solar array temperatures and convective heat flux) gives the capability to autonomously command a safeguard action in case of exceeded threshold on such parameters. This is extremely valuable when the ground has not enough time to react before the next periapsis pass at the end of aerobraking, in particular in case of dust storm. Eventually, a new safe mode is proposed that copes with the specificities of the aerobraking phase, removing the need for costly pop-out maneuvers while guaranteeing spacecraft safety. This safe mode combines a low-drag configuration (with the solar arrays edge-on into the flow) with a pop-up ΔV for increased thermal protection.

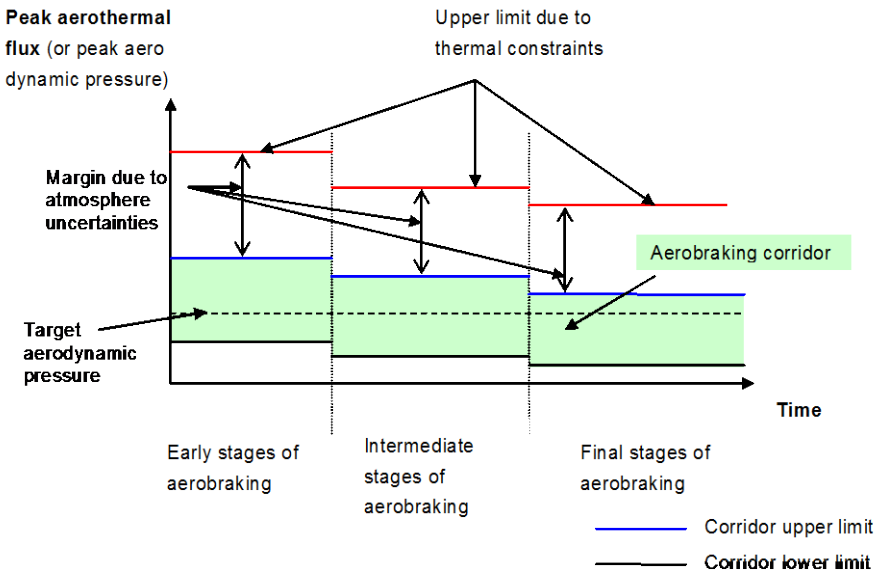

Figure 2: Aerobraking corridor ; as aerobraking progresses, the corridor upper limit decreases as the orbit becomes more circular and drag passes last longer

2. Mission scenario

Based on ESA inputs and requirements, a system trade-off analysis allowed determining the operational point for the autonomous aerobraking scenario, which consists in the baseline characteristics of the satellite and the orbit which have been considered during the study.

The case considered is based on the MarsGEN spacecraft whose design is an output of an ESA system study performed in 2009. It is a Mars network science mission, due for launch in 2020 or 2022. Given a ballistic coefficient of 25 kg/m² for the MarsGEN spacecraft, a trade-off between aerobraking strength, aerobraking duration and initial apoapsis altitude was made. It led to an initial orbit apocentre altitude at 67500 km (the final orbit is circular at 508 km) and a target peak dynamic pressure of 0.5 N/m². In these conditions, aerobraking duration is limited to six months.

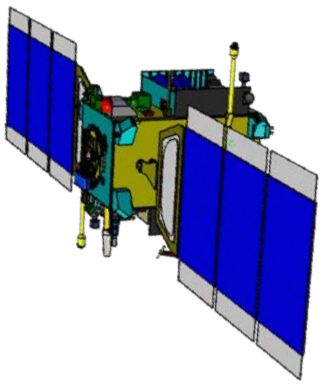

Figure 3: Illustration of MarsGEN spacecraft

3. High-Fidelity Aerobraking Simulator (HiFAS)

A High-Fidelity Aerobraking Simulator (HiFAS) was developed in order to implement, validate and evaluate the designed autonomous aerobraking strategies, with special features including accelerated simulations and high-fidelity environment modelling.

Validation of aerobraking strategies requires simulations that cover full orbits, meaning that a single simulation will include periapsis passes, i.e. short periods of rapidly changing dynamics, but also long periods with very slow dynamics outside of the atmosphere. For fast end-to-end simulations, Astrium Satellites implemented an efficient solution to manage the various frequencies in the same simulator, thanks to an architecture where scheduling is completely managed by the model (Variable Scheduler), considerably improving simulation time.

Environment modelling includes high-fidelity Mars atmospheric models (mean MarsGRAM 2001, Global Circulation Model, Mars Climate Database - MCD) that provide with atmospheric density at any location around Mars. It also includes a 20x20 Mars gravity model, solar gravity, and solar radiation pressure. Combined with a refined aerodynamic model of the MarsGEN orbiter spacecraft that accounts for the transitional regime of the airflow, forces and torques applying to the spacecraft are accurately computed at each time step. Temperatures are also computed on five different locations on the spacecraft, based on a thermal model of the spacecraft and taking into account the convective heat flux due to atmospheric drag and radiative heat fluxes including solar, Mars albedo and Mars infrared contributions.

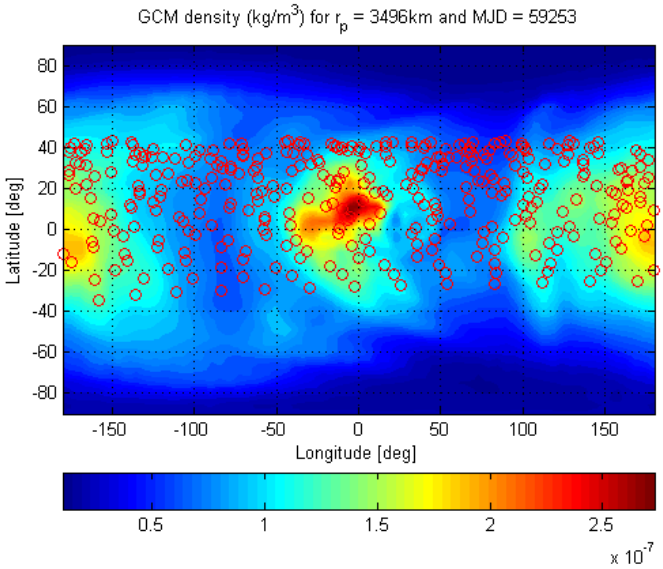

Figure 4: Atmospheric density over the surface of Mars as provided by the Global Circulation Model for a given date and distance to Mars centre ; red circles indicate locations of periapses over the aerobraking phase

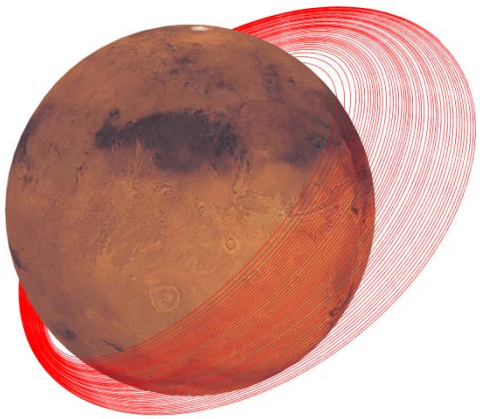

Figure 5: Illustration of the final part of the aerobraking trajectory as computed by HiFAS

4. AOCS mode for aerobraking

The first step to design autonomous aerobraking strategies lies in the definition of the AOCS mode for aerobraking since it drives any autonomy requirement. An aerobraking orbit is made up of two distinct phases. Firstly a vacuum phase with very low perturbations and where pointing strategy and AOCS are driven by system level needs (e.g. power, thermal). Secondly an atmospheric phase with high perturbations and where pointing strategy and AOCS are driven by aerodynamic conditions. Due to these very different environmental conditions, two different modes are needed over an aerobraking orbit. Building upon the Astrium Mars Express and Venus Express experience [3], detailed trade-offs have been performed regarding attitude guidance, control and estimation options for the atmospheric phase and a set of criteria including spacecraft controllability, propellant consumption, robustness, complexity, and impacts on onboard navigation.

These trades led to the following baseline for the Aerobraking Mode AOCS:

- Attitude estimation is based on gyro propagation;
- Attitude guidance is constant in inertial space from the beginning until the last stage of aerobraking (typically one to two weeks) where it becomes time-varying, following the orbital velocity vector direction;
- Attitude control is a thruster-based, wide deadband phase-plane controller, with a variable control torque in pitch and yaw, and a fixed control torque in roll.

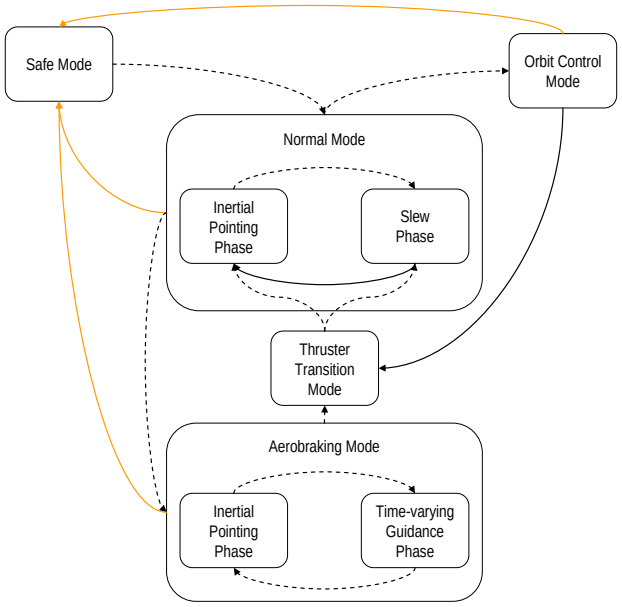

Figure 6: AOCS architecture

The Normal Mode is the standard Astrium Satellites normal mode for interplanetary missions, based on gyrostellar attitude estimation and reaction wheels for attitude control. The transitions between Normal Mode and Aerobraking Mode are commanded by AOCS sequences. Up to now, these sequences have been generated by ground operations and regularly uplinked to the spacecraft.

The guidance function is in charge of computing the attitude profile at any time (reference quaternion) from the current time and the information included in the current sequence. Both time-varying and inertial (see Figure 7) guidance schemes are used, based on the following rationale:

- At the beginning of aerobraking, the direction of the orbital velocity vector does not vary much through the atmospheric pass, so that the reference attitude quaternion may be considered constant. It is taken aligned with the orbital velocity direction at periapsis;
- At the end of aerobraking, the orbit is close to circular and the spacecraft spends a large part of each orbit within the atmosphere, so that the direction of the orbital velocity vector varies significantly through the pass; therefore the reference attitude quaternion must be considered time-varying.

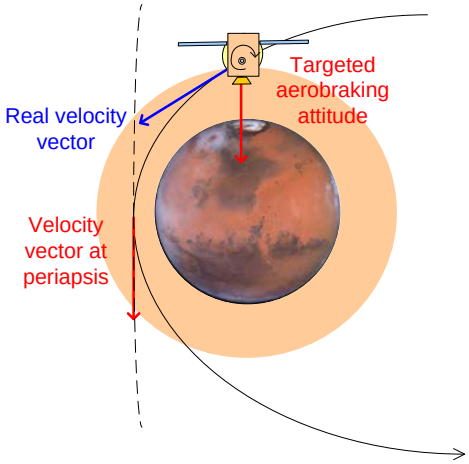

Figure 7: Inertial attitude guidance over one atmospheric pass ; at the beginning of aerobraking (dashed line), the direction of velocity varies much less than at the end (solid line)

The benefits of using an inertial guidance scheme are twofold: firstly, it is obviously simpler to implement, and secondly, it is more robust to timing errors than the time-varying guidance scheme. This is all the more important that timing errors may be more important at the beginning of aerobraking, when the prediction of the time of next periapsis is highly sensitive to the drag ΔV, which is difficult to predict on the ground due to atmospheric density variability. The transition from inertial guidance to time-varying guidance is done on the ground. It is chosen so that the off-pointing between orbital velocity at atmospheric entry / exit and velocity at periapsis is about 15 deg. For MarsGEN reference scenario, this leads to a transition occurring 5 days only before the end of aerobraking, meaning that time-varying guidance becomes necessary only for the very last few days of aerobraking.

Regarding attitude control during atmospheric passes, all aerobraking missions exhibit a configuration that is aerodynamically stable. This is illustrated by the Mars Express / Venus Express configuration shown on Figure 8. Any non-null angle of attack will induce a restoring aerodynamic torque, thanks to the rear-shifted solar array attachment point. As considered before [3] [4], the chosen approach is then to rely on this aerodynamic stability in order to save propellant, so that a simple deadband phase plane controller using AOCS thrusters is used in order to avoid excessive attitude and/or rate errors. The deadband is taken rather wide, at 15 deg for attitude and 2 deg/s for rates.

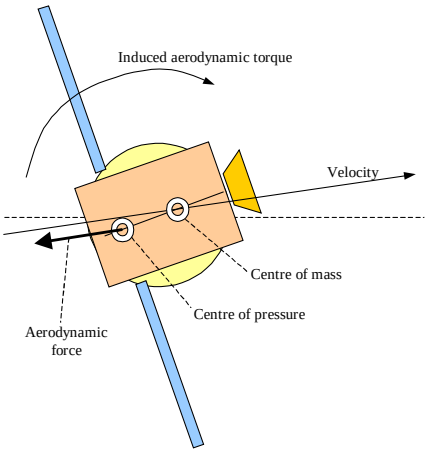

Figure 8: Aerodynamic stability on Mars Express

The aerobraking mode AOCS was the subject of dedicated simulation scenarios on HiFAS. The proposed design was tested on three different orbit cases covering the whole six month long aerobraking phase (aerobraking start, middle and end), and with nominal or shifted AOCS sequences in order to evaluate the robustness of the design to timing errors experienced in flight. Typical simulation plots of the difference between the commanded attitude and the actual one are shown in Figure 9 hereafter for illustration:

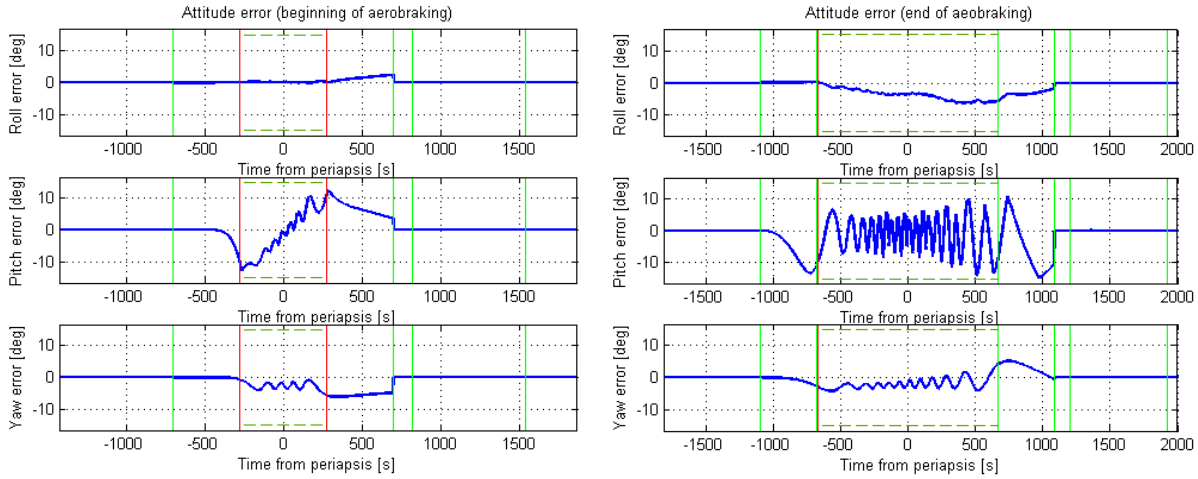

Figure 9: Attitude error (depointing) for two atmospheric passes (left-hand side: beginning of aerobraking; right-hand side: end of aerobraking)

Note the attitude oscillations due to the initial angular offset and the aerodynamic restoring torque. At the beginning of aerobraking, the ramp effect is due to the inertial guidance scheme. In both cases, only a few thruster pulses are fired, at the end of the atmospheric pass when the spacecraft exits the atmosphere and tends to reach the deadband limits. The discontinuity occurring at the end of the atmospheric pass is due to the transition to Thruster Transition Mode (TTM), which aligns the commanded attitude with the current attitude. The attitude guidance and control design for the aerobraking mode was validated, for both nominal aerobraking operations and safe mode operations (see §7 below). In particular the inertial guidance approach taken at the beginning of aerobraking has been validated, thus relaxing timing constraints. Consumption remains reasonable, however additional activities could be performed on controller tuning. Windmill torque roll control may be a significant component of the attitude control consumption, so it is recommended to minimize solar array misalignment – or use it for roll control.

5. Autonomy level 1

As discussed above, the general approach chosen for attitude guidance and control is simple and has not been fundamentally modified since Magellan, the first aerobraking mission (around Venus), although some alternative approaches have been discussed in R&D studies. Traditionally, attitude guidance during each pass has been based on a time-varying profile that aims at following the direction of orbital velocity, so that the spacecraft remains aligned with the relative airflow. It is then sensitive to uncertainties in orbit timing, as any timing error translates immediately into an angular error, which should be minimized in order to avoid any ergol overconsumption or dangerous spacecraft configuration w.r.t. the airflow. In past US missions, timing errors had to be kept lower than typically 225s, which is challenging with atmospheric density prediction errors of about 35% (1σ) [5]. The results shown on Figure 9, based on a simplified aerobraking setup and orbit propagation model, show how such a level of atmospheric variability is quickly degrading the knowledge in the timing of consecutive orbits. Since the timing error accumulates over consecutive orbits in a single sequence, the maximum length of each sequence is constrained by the maximum timing errors acceptable for the last orbit. Fortunately, the effect of atmospheric variability is most important for long period orbits i.e. when the ground is still able to construct a new sequence at each orbit. As the orbit shrinks and it is increasingly difficult for the ground to construct a new sequence for each orbit, the effect of atmospheric variability also decreases and it becomes possible to include additional orbits in the same sequence without exceeding the timing error constraint. However, the pressure on the ground remains high, with a need to build and uplink new drag sequences up to 4 times a day. It becomes apparent that a certain level of autonomy is needed in order to supplement ground operations, in particular after the orbital period has decreased under a critical duration. These results are confirmed by flight experience from US missions [6]. The main objective of raising the autonomy to level 1 is to relax this pressure on the ground. Indeed, sequences generated by the ground and uplinked to the spacecraft can be corrected on-board thanks to measurement of key aerobraking events and parameters: detection of atmospheric entry, estimation of periapsis pass date, heat flux, atmospheric drag ΔV. These data can be down-linked to the ground or used onboard to correct sequences accordingly to actual orbit events when it becomes necessary.

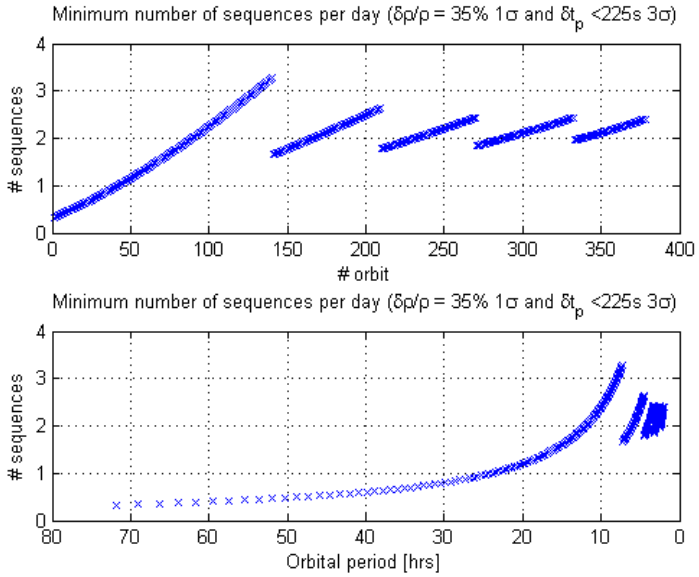

Figure 10: number of sequence builds per day (on top: against orbit number; below: against the orbital period)

As a conclusion, AOCS sequence (i.e. the list of transitions from one AOCS mode to the next with the appropriate dates) timing is difficult when performed on the ground because of the unavoidable atmospheric variability combined with an ever shortening orbital period and limited ground response time. Therefore the first step for raising the autonomy level is to provide the spacecraft with autonomous drag sequence shift capability. The main objective is to reduce the frequency of drag sequence builds to a maximum of one per 24 hours, with a goal of one sequence uplink every three days on average.

In order to meet this performance, an onboard algorithm called Periapsis Time Estimator (PTE) capable of keeping timing errors below a given threshold (420s with inertial guidance, then down to 180s with time-varying guidance) throughout the aerobraking phase was proposed and designed, based on onboard detection and prediction of times of periapses. The most straightforward way of detecting the time of periapsis passage is to use drag acceleration measurements based on onboard accelerometer, the time of maximum drag being close to the time of periapsis passage. The proposed algorithm not only measures the date of periapsis but also computes an updated orbital period from the integrated ΔV effect of drag in order to predict the time of next periapsis, as this effect was shown to be significant for long period orbits.

The algorithm works as follows. After periapsis pass P_n, the date of periapsis $t_{P,n+1}$ is estimated from the measured date of periapsis $t_{P,n}$ and the estimated orbital period of orbit n T_n, which is itself computed from the orbital period of orbit n-1 plus the change in orbital period that is due to atmospheric drag at P_n:

$$\begin{cases} T_n = T_{n-1} + \Delta T_n \\ t_{P,n+1} = t_{P,n} + T_n \end{cases} \quad \textbf{(1)}$$

The orbital period change ΔT_n is computed from semimajor axis change Δa induced by the total drag ΔV:

$$\Delta a_{drag} \approx \frac{2}{n^2 a} v_P \int_{drag} a_T(t)dt = \frac{2}{n^2 a} v_P \cdot \Delta V_{drag} \quad \textbf{(2)}$$

Where v_P is the velocity at periapsis, a_T the tangential acceleration, n the orbit mean motion and a the semimajor axis. Note that the formula above assumes that drag applies instantaneously and entirely at periapsis. This assumption is made in order to facilitate the processing of accelerometer measurements. However, the difference between the orbital period changes given by the exact computation (non-instantaneous drag ΔV) and the simplified method

(instantaneous drag ΔV) can be as high as 4.5%. The resulting error on the orbital period change may be quite large at the beginning of aerobraking, and consequently it has been chosen to simply correct the orbital period change obtained from the "drag impulse" assumption by a constant correction factor, taken at 0.955, greatly improving the performances of the PTE. The application of a constant factor becomes detrimental to the accuracy of the orbital period change computation below a certain orbital period (~25 hours), where it may simply be deactivated (i.e. set to 1). The PTE principles are summarized on Figure 10 hereafter. The PTE is completed by a sequence shifting function that updates future drag sequences based on the predicted time of next periapsis computed by the PTE.

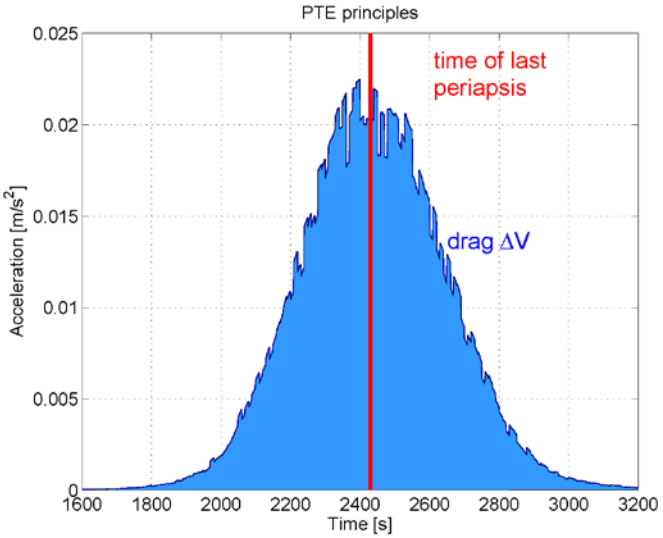

Figure 11: PTE principles; after each drag pass, the time of next periapsis is computed from the time of last periapsis and the drag ΔV integrated over the drag pass

The performances of the PTE have been assessed over one atmospheric pass and over three days, fulfilling the requirements on prediction of time of next periapsis expressed above. Furthermore, its robustness to atmospheric short-scale variability has also been demonstrated using the MCD atmospheric model. Two examples of perturbed atmospheric density profiles are shown on Figure 12, while PTE performances for 100 runs are shown on Figure 13, showing that the specifications are met very well, including on realistic density profiles. The PTE has been validated over the target autonomy horizon, enabling autonomous sequence shift over 3 days. Its robustness to long-scale and short-scale atmospheric perturbations has been demonstrated. One of the main lessons learned was that the implementation of a corrective factor to account for non-instantaneous drag ΔV was required. Calibration of accelerometers bias before atmospheric passes may also be necessary at the beginning of aerobraking.

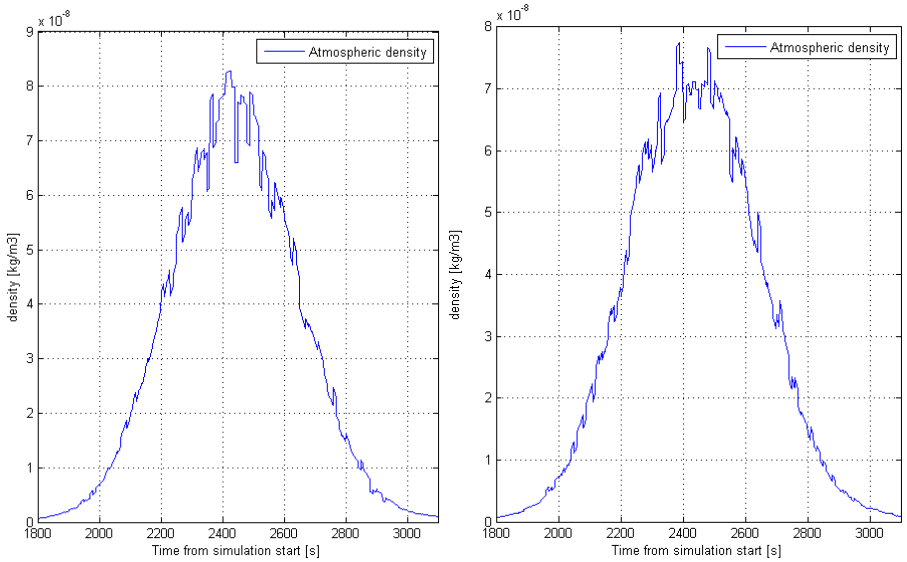

Figure 12: Perturbed atmospheric profiles

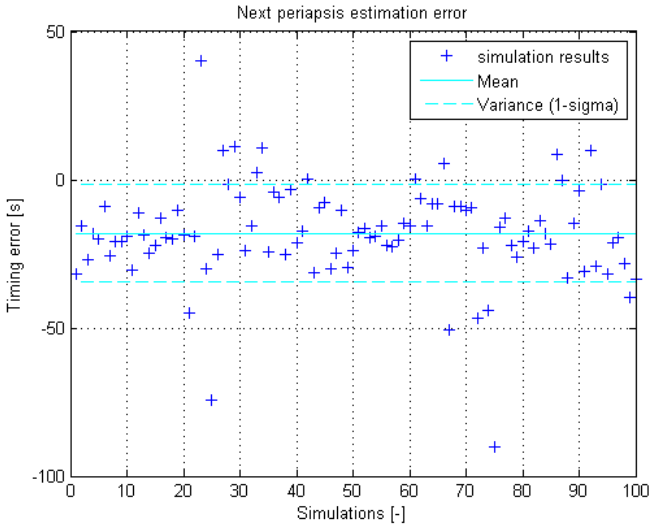

Figure 13: Next periapsis statistical estimation error (end of aerobraking)

6. Autonomy level 2

In autonomy level 2, the main goal is to extend the spacecraft autonomy to a duration of one week. The underlying objective is to relieve the ground from most low-level activities, so that it may focus on high-level activities. Two activities were considered for onboard implementation: drag sequences building and corridor control (i.e. boost maneuver analysis, decision-making and selection). In all cases it was assumed that the ground still performed regular orbit determination and high-level activities including atmosphere monitoring and trending, updates to atmospheric and thermal models, aerobraking progress monitoring and aerobraking corridor updates.

Generating drag sequences requires knowing the direction of the velocity vector through the atmospheric pass, or at least at periapsis (depending if the guidance is time-varying or inertial). The direction of the velocity vector may be inferred from orbital elements (a, e, i, Ω, ω) which evolve differently over the aerobraking phase. A trade-off for navigation was performed, and led to the simplest option able to answer the aerobraking needs: onboard estimation of a and e, and rely on ground updates for (i, Ω, ω). This approach is justified by the fact that while a and e are impacted at first order by atmospheric variability and must therefore be estimated onboard, this is not true any longer for (i, Ω, ω) that are impacted at first order by deterministic effects (e.g. Mars gravitational field), so that their evolution may be predicted by the ground in advance with sufficient accuracy. In order to validate this approach, the evolutions of “ground-based” models of (i, Ω, ω) based on a simplified gravity model and simple, exponential atmospheric model are compared with “true” values, based on a 20x20 gravity model and GCM density. Typical evolutions are shown on Figure 14:

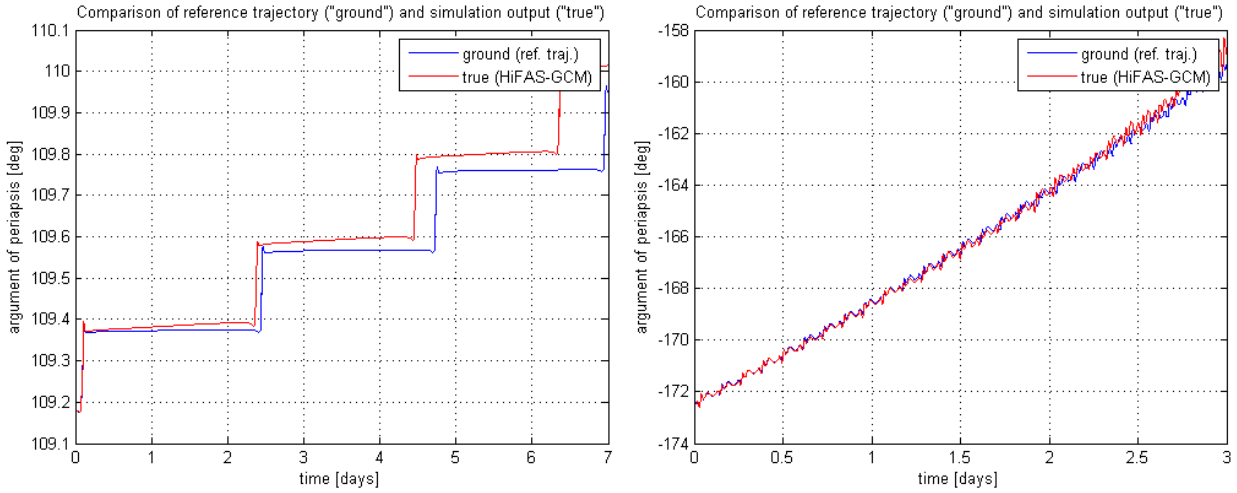

Figure 14: Example of orbital parameter errors (argument of periapsis), for the start and end of aerobraking

At the start of aerobraking, the differences between the two evolutions after propagation over one week remain very small and are actually negligible. At the end of aerobraking, Ω and ω evolve faster due to gravitational perturbations as the spacecraft is much closer to Mars. Errors on Ω and ω are not negligible any longer; however they remain acceptable over a horizon of 3 days (instead of one week). This navigation strategy is validated, as long as sufficiently frequent orbit determination is performed by the ground at the end of aerobraking.

Regarding autonomous corridor control, a trade-off was performed on a selected set of reactive (based on measured, i.e. past, heat fluxes) and predictive (based on predicted, i.e. future, heat fluxes) strategies. While predictive strategies show slightly better performances, this trade-off has shown that it is possible to design reactive strategies with a reasonable ΔV usage while respecting thermal constraints, at the expense of a slightly degraded but still acceptable aerobraking efficiency. Reactive strategies being much less complex to develop, implement, tune and validate than predictive ones, and consequently preferable from a system-level perspective, such a strategy was implemented in the baseline. The autonomous corridor control was validated and evaluated at the start, middle and end of aerobraking. The simulations cover 7 days which is the target autonomy horizon of level 2 (except for the end case, where the end of the aerobraking main phase is reached slightly earlier). Illustrations of the heat flux evolution during these simulations and its comparison with the aerobraking corridor are provided in Figure 14 below.

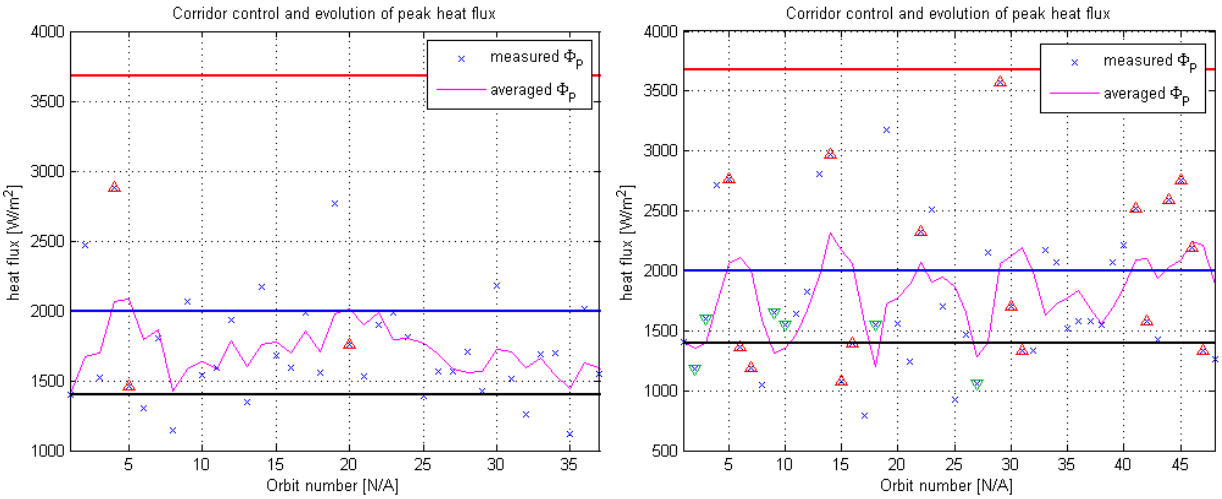

Figure 15: Heat flux evolution during autonomous corridor control (aerobraking middle and end cases) ; upwards, red triangles indicated periapsis up maneuvers, and downwards, green triangles indicate periapsis down maneuvers.

In both cases, the autonomous corridor control strategy is able to ensure thermal safety while maintaining a sufficient level of drag. Regarding autonomy level 2, the feasibility of the simple approach for autonomous corridor control (minimal onboard navigation, simple heat flux control) has been demonstrated over the target autonomy horizon,

potentially removing the need for complex onboard propagator, models, and fully autonomous navigation. The frequency of the required ground updates to support onboard navigation has been preliminary estimated (from > 7 days to ~3 days in the end).

Heat flux measurement is provided by the Aerothermal Monitor, which computes the heat flux experienced by the spacecraft at the last atmospheric pass. Firstly the drag acceleration at the center of mass is computed from acceleration measurements, gyro measurements, thruster firings history (e.g. for attitude control). Then the dynamic pressure profile is computed from the longitudinal component of the acceleration due to drag (best signal-to-noise ratio). In order to retrieve dynamic pressure and density from the acceleration, it is required to know the axial force coefficient C_z, which depends on the Knudsen number *Kn* (i.e. on density) and on the aerodynamic flux direction in spacecraft frame. The sensitivity of C_z to the attack and sideslip angles being very low when they are below 10 deg (which is the case for aerobraking trajectories), only an estimate of *Kn* is needed. However *Kn* depends on density which is unknown. In order to solve this problem an iterative approach is chosen, initiated with a first C_z value corresponding to free-molecular regime (i.e. *Kn* = 10) and repeated until density values converge. Once density and dynamic pressure are estimated, heat flux is then computed assuming a constant velocity (velocity at periapsis), and a reasonably conservative value for the convective heat transfer coefficient C_H.

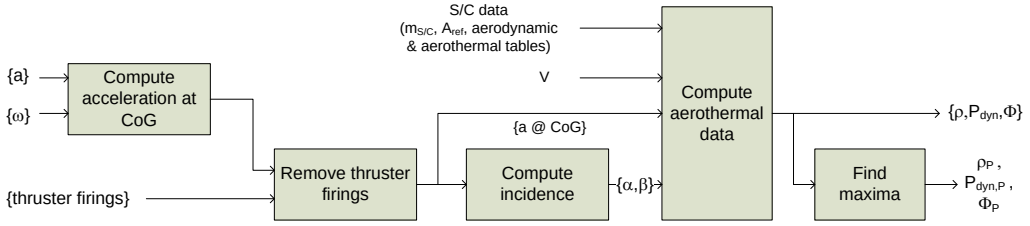

Figure 16: Aerothermal Monitor

The performances of the Aerothermal Monitor were shown to be good enough for the identified needs. They could be further improved with a better knowledge of the spacecraft aerothermal coefficient C_H and estimation of the airflow velocity, by taking winds into account.

7. Contingencies and aerobraking safe mode

In the frame of this study, focus was put on two main contingency cases, shown to be the most critical from flight experience: unsafe thermal situation, and a switch to safe mode.

In order to react to an excessive temperature and/or heat flux and ensure thermal protection, an Immediate Action Manager (IAM) has been designed. When thermal variables (peak heat flux or temperature) exceed a pre-defined threshold, a ΔV boost is performed at the following apoapsis. The temperature and heat flux thresholds have been derived from thermal analyses, and the pop-up ΔV has been sized so that a significant density decrease is experienced by the spacecraft at the next periapsis pass, while keeping in mind propellant consumption constraints. The Immediate Action procedure was validated, reducing the experienced temperatures at the next periapsis even in the case of a global dust storm. However, the IAM procedure being a reactive process, the maximum temperature may be exceeded once during a global dust storm. This may be acceptable as it only lasts for a short duration, but at least delta-qualification of equipments and/or ground support is recommended, in particular at the beginning of aerobraking.

Classical safe mode for interplanetary spacecraft leads to a Sun / Earth pointing attitude which could lead to high temperature on solar cells or other spacecraft equipment, unexpected attitude variations due to aerodynamic disturbances and uncontrolled braking during up to several days until spacecraft recovery. It appeared necessary to develop a safe mode for the aerobraking phase that answers all classical safe mode requirements (i.e. simple, robust, and requiring a minimal amount of context information) but also puts the spacecraft in a safe configuration with respect to the air flow during atmospheric passes and limits drag-induced orbit degradation until spacecraft recovery by the ground. Several options were identified for safe mode during the aerobraking phase, and a trade-off was performed against a set of criteria including complexity, spacecraft safety, orbital decay, ΔV cost, impacts on navigation. It led to the choice of a low-drag safe mode with the solar arrays edge-on to the flow combined with a pop-up ΔV for MLI thermal protection.

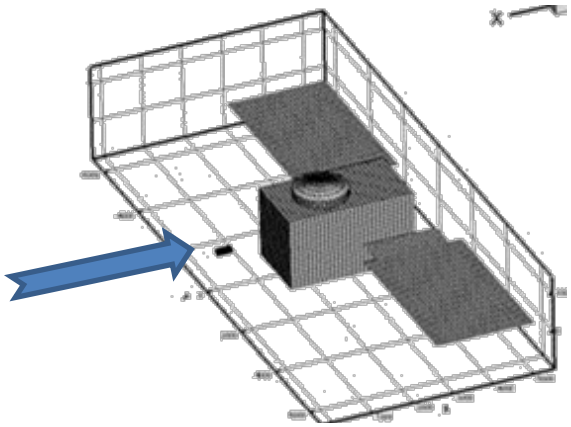

Figure 17: Aerobraking safe mode configuration, with solar arrays edge-on to the flow

Both short-term (over one atmospheric pass) and long-term (over two days) aspects of the aerobraking safe mode are considered in the strategies validation plan. The following plots illustrate the evolution over two days of two critical metrics (battery charge and orbital decay) after safe mode trigger, showing that the proposed safe mode correctly fulfils the needs.

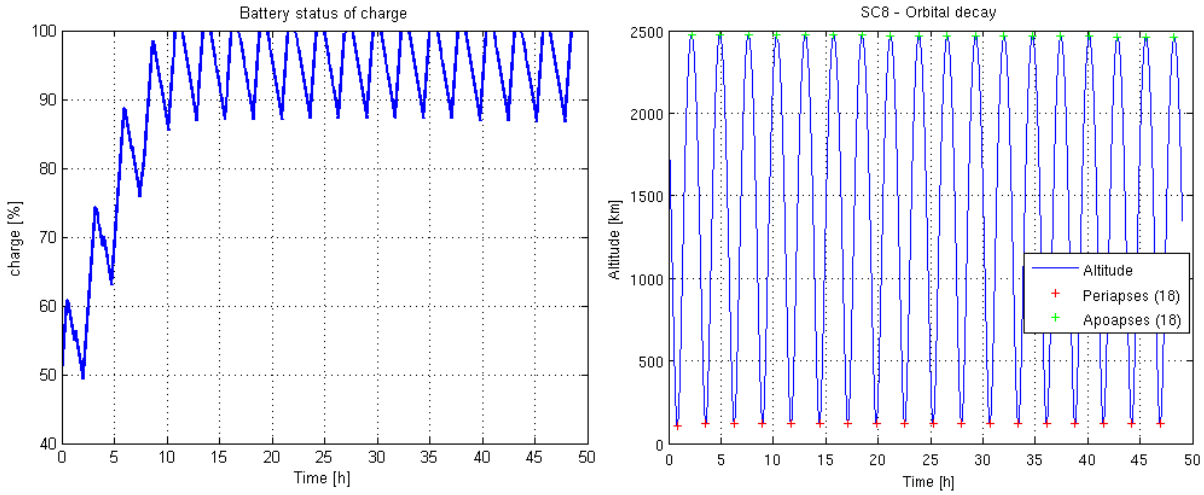

Figure 18: Battery state of charge and orbital decay while in safe mode, at the end of aerobraking

The proposed aerobraking safe mode design has been validated by simulations, ensuring spacecraft safety. As the timing of ground-computed safe mode sequences is shifting over two days, longer timing margins are needed and this may become a battery sizing driver (alternative but more complex solutions have also been identified).

8 Conclusion

Several major achievements towards a more autonomous and more robust aerobraking have been presented. Firstly, the proposed AOCS design for aerobraking has been validated, including an innovative guidance scheme that not only is simpler in terms of onboard implementation, but also allows robustifying aerobraking to atmospheric variability. The PTE has been validated over realistic atmospheric density profiles, enabling autonomy level 1 for future European missions and bridging the gap with US missions. Regarding the more advanced autonomy level 2, the feasibility of the proposed simple approaches to onboard navigation and autonomous corridor control has been demonstrated. An innovative safe mode design has been proposed and validated by simulations, ensuring spacecraft safety at a low ΔV cost. At last, the immediate action procedure triggered in case of thermal alarm was validated, reducing the experienced temperatures at the next periapsis, even in the case of a global dust storm. The natural way forward is to validate and evaluate the proposed autonomy algorithms on actual flight data. In particular, the Venus Express aerobraking experiment considered for 2014 would be a great opportunity for a first demonstration of their operational capabilities [7].

References

[1] Spencer, D., and R. Tolson. 2007. Aerobraking Cost and Risk Decisions. In Journal Of Spacecraft And Rockets Vol. 44, No. 6, November–December 2007
[2] Johnson, M. A., and W. H. Willcockson. Mars Odyssey Aerobraking: the first step towards autonomous aerobraking operations.
[3] Régnier, P., E. Ecale, S. Val Serra. 1999. AOCS design for scientific missions Rosetta / Mars Express. 4th ESA International Conference on Spacecraft Guidance, Navigation and Control Systems. ESTEC, Noordwijk, the Netherlands.
[4] Beerer, J. et al. 1996. Aerobraking at Mars: the MGS Mission. 34th Aerospace Sciences Meeting & Exhibit
[5] Lyons, D. T. 1999. Aerobraking at Venus and Mars: a comparison of the Magellan and Mars Global Surveyor aerobraking phases. AAS 99-358
[6] Gladden, R. E. 2009. Mars Reconnaissance Orbiter: Aerobraking Sequencing Operations and Lessons Learned. Space Operations Communicator Vol. 6, No. 1, January — March 2009
[7] Val Serra, S. et al. 2011. Venus Express Aerobraking. 18th IFAC World Congress.